Journal of Engineering and Development, Vol. 17, No.2, 2013, ISSN 1813- 7822

A Theoretical Comparison of a Combined Ejector–Absorption Refrigeration System with a Conventional absorption system

Dr. Adnan M. Al – Saffawi
Ass. Professor
Dep. of Mech. Engg. / Univ. of Mosul

Ahmed M. Al – Hasani
M.Sc.
Dep. of Mech. Engg. / Univ. of Mosul

Abstract

This paper presents a mathematical model which has been built to design a combined ejector-absorption refrigeration system, as well as another mathematical model built to design a conventional absorption refrigeration system. Both of these models use lithium Bromide-water as a working solution. The Engineering Equation Solver (EES) Software has been used to perform the mathematical analysis and the design. A comparison of the results for both of the absorption systems for a cooling capacity of (5 Ton) has been done at the same operation conditions, which was obtained from the simulation of the conventional absorption to optimize the system performance, represented by (40.41°C) condenser temperature, (9°C) evaporator temperature and (36.12°C) absorber temperature. But the generator temperature was different for both of the systems. The coefficient of performance obtained was (0.7871) for the conventional absorption refrigeration systems at the generator temperature of (81.94°C), while the value of coefficient of performance was (1.026) for the proposed absorption system at the generator temperature of (200.5°C) which is higher than the coefficient of performance for conventional absorption refrigeration system by about (30.35%) .

Keywords: Refrigeration System , absorption , water-lithium bromide solution , ejector , COP , design .

مقارنة نظرية لمنظومة مركبة من قاذف حراري مندمج داخل منظومة التبريد الامتصاصية مع منظومة امتصاصية تقليدية

أ.م.د. عدنان محمد الصفاوي
قسم الهندسة الميكانيكية/جامعة الموصل

أحمد مؤيد الحسني
قسم الهندسة الميكانيكية/جامعة الموصل

الملخص

يتضمن البحث بناء نموذج رياضياتي لتصميم منظومة مركبة من قاذف حراري مندمج داخل منظومة التبريد الامتصاصية فضلاً عن نموذج آخر لتصميم منظومة تبريد امتصاصية تقليدية وكلاهما يستخدم محلول (بروميد الليثيوم-ماء) كمحلول تشغيلي . ولتنفيذ التحليل الرياضياتي والتصميم استخدم برنامج (EES) Engineering Equation Solver . تمت مقارنة نتائج كلا المنظومتين الامتصاصيتين لسعة التبريد (5 Ton) وعند نفس الظروف التشغيلية التي تم الحصول عليها من محاكاة المنظومة الامتصاصية التقليدية عند أفضل أداء للمنظومة والمتمثلة ب (40.41) درجة مئوية للمكثف و(9) درجة مئوية للمبخر و(36.12) درجة مئوية لوعاء الامتصاص. أما درجة حرارة المولد فهي مختلفة في كلا المنظومتين , وقد تم الحصول على معامل أداء (0.7871) في منظومة التبريد الامتصاصية التقليدية عند (81.94) درجة مئوية للمولد , بينما كانت قيمة معامل الأداء (1.026) في المنظومة الامتصاصية المقترحة عند (200.5) درجة مئوية للمولد وهو أعلى بحوالي (30.35 %) عن معامل الأداء الخاص بمنظومة التبريد الامتصاصية التقليدية.

Nomenclature

a	Cross sectional area.	m^2
A	Surface area.	m^2
COP	Coefficient of performance.	-------
C_p	Specific heat at constant pressure.	$kJ/kg\ .K$
D	Diameter.	m
d_x	Lithium bromide strong-weak solution concentration differences.	-------
G_t	Refrigerant mass flux through the throat of the nozzle.	$kg/m^2.s$
G_{sy}	Secondary refrigerant mass flux to the constant area chamber.	$kg/m^2.s$
h	Enthalpy.	J/kg
k	Heat capacity ratio $=C_p/C_v$.	-------
L	Length.	m
L_d	Length of the diffuser.	m
M	Mach number.	-------
$\dot{m}$	Mass flow rate.	kg/s
P	Pressure.	N/m^2
Q	Heat energy.	W
R	Gas constant.	$J/kg.K$
T	Temperature.	K
T_{crit}	Critical lithium bromide strong solution temperature.	K
T_{pinch}	Minimum temperature difference between the hot and cold curves.	K
U	Overall heat transfer coefficient.	$W/m^2.K$
V	Fluid velocity.	m/s
v	Specific volume of the fluid.	m^3/kg
W_{pump}	Work input to the pump.	W
X	Solution concentration.	-------

Greek symbols

ε	Effectiveness.	-------	θ_3	Diverging diffuser angle.	*Degree*
η	Efficiency.	-------	ρ	Density.	kg/m^3
θ_1	Converging nozzle angle.	*Degree*	ω	Entrainment ratio.	-------
θ_2	Diverging nozzle angle.	*Degree*	ΔT_m	Log-mean temperature difference.	*K*

Subscripts

1,2…	Condition at state.	*m*	Mixing.
a	Absorber.	*N*	Nozzle.
c	Condenser.	*p*	Primary stream.
d	Diffuser.	*pump*	Solution pump.
e	Evaporator.	*s*	Secondary flow, steam.
g	Generator.	*shx*	Solution heat exchanger.
i	Point at the nozzle outlet.	*strong*	Lithium bromide strong solution.
is	Isentropic state.	*t*	Throat of the nozzle.
j	Point at the diffuser inlet.	*w*	Water.
k	Throat of the diffuser.	*y*	Section (y-y).

1. Introduction

There are several heat powered refrigeration systems such as adsorption system, ejector system, and absorption system. Of the three types of heat powered system , the absorption refrigeration system is considered to be the best in terms of energy performance and it is environmental suitable , which works with different heat sources such as steam , electric heaters or by burning the natural gas and light oils , solar energy or geothermal energy . It consumes a small amount of a mechanical work by its pump. It is also quiet and vibrationless . As well as the working fluid of this systems (lithium bromide-water , ammonia-water) are environmentally friendly which have no threat to global environmental ozone depletion and may have less impact on global warming and these working fluids are available commercially. The real problems for water-lithium bromide systems are: crystallization and corrosion when the solution concentration and the temperature are high. Current commercial available lithium bromide absorption refrigeration systems are not suitable for working at a solution concentration greater than (65%) and a solution temperature greater than (200)°C because of crystallization and corrosion and this problem inevitably reduces the efficiency of the system when using high temperature heat sources [1] .

An ejector is a device which utilizes the momentum of a high – velocity jet vapour to entrain and accelerate a slower moving medium into which it is directed. The resulting kinetic

energy of the mixture is subsequently used for self compression of the substance to a higher pressure in the device, which thus fulfills the function of a compressor. It is used instead of a compressor in a vapour-compression system. To treat the crystallization problem which may occur in the conventional absorption refrigeration system (**CARS**) at high temperature and high concentration for a strong lithium bromide solution. An ejector – absorption refrigeration system (**EARS**) has been developed and tested by researchers in recent years.

Zong – Chang and Jian – Wei (2008)[2] Proposed a novel ejection – absorption heat pump by adding an ejector between the generator and condenser in absorption cycle used a lithium bromide – water as a working fluid . Based on the theories about ejector and absorption cycle, the thermodynamic performances of this novel ejection – absorption heat pump are simulated in details. Researchers calculated the coefficient of performance (**COP**) and entrainment ratio of ejector under different conditions. They also analyzed the effects of entrainment ratio, condensation, evaporation and generation temperatures on the coefficient of performance and exergetic efficiency . When compared the results with a conventional absorption heat pump, the coefficient of performance of the novel heat pump is increased obviously, while system complexity is increased a little.

Ereira (2009)[3] studied the use of a liquid-vapour ejector without phase change for the pressure recovery in the absorption refrigeration system , where the ejector was installed at the absorber inlet in a single-stage absorption cycle working with a low temperature heat source and an ammonia-water mixture , therefore converting the cycle into an advanced three pressure level ejector – absorption cycle (**TPL**) . He developed and applied a new two – phase flow model for the liquid – vapour ejector as a simulation program in order to find the possible pressure recovery and respective ejector design, within the desired cycle's working conditions. It was found that the pressure recovery increases for lower diffuser angles, with a maximum pressure recovery of **(0.05)**bar for a tube of (**20**)cm length .

Daliang Hong et al (2010)[4] simulated a novel ejector – absorption combined refrigeration cycle . When the temperature of heat source is high enough, the cycle worked as a double – effect cycle. They noted that, if the temperature of heat source is lower than the required temperature of the heat source used to drive conventional double – effect absorption refrigeration cycle but much higher than required temperature of heat source used to drive

conventional single – effect absorption refrigeration cycle. The results showed that the coefficient of performance of a new cycle will be higher than that of the conventional single – effect absorption refrigeration cycle. Where the simulation results showed that the coefficient of performance of the cycle is (30%) higher than that of the conventional single – effect absorption refrigeration cycle at the condensing temperature and absorption temperature of (40)°C , evaporation temperature of (5)°C and the temperature of the heat source was higher than (122.5)°C . Also they showed that the relative increasing ratio was increased as the temperature of the heat source increases. When the temperature of heat source reaches to (130)°C, the relative increasing ratio is higher than (10)% , when it reaches to (136)°C , the relative increasing ratio is higher than (20)% , when it reaches to (142)°C , the relative increasing ratio is higher than (30)%. When the temperature of the heat source is higher than (150)°C , new cycle will work as a double – effect cycle .

2. Proposed refrigeration system

The proposed refrigeration system is an absorption refrigeration system using a lithium bromide – water as a working solution. It contains an ejector between generator and condenser and using the thermal energy as a heat source in order to produce a saturated steam in the generator. Referring to the **figure(1)** the lithium bromide – water solution is heated in the generator by heat source in order to produce a very high – pressure steam refrigerant at state point**(1)** . This steam (primary fluid) expands when flows through the convergent – divergent nozzle of the ejector shown in **figure(2)** , accelerated to a high velocity stream and reaches a supersonic velocity at the exit of the nozzle producing a low pressure at state **point(i)** , the low pressure caused by this expansion induces vapour (secondary fluid) from the evaporator at state **point(13**) . The two streams are mixed in the mixing chamber and enter the diffuser where most of the remaining velocity head is converted back to pressure. The pressure rise is accompanied by a rise in temperature, and when the vapour moves into the condenser, heat begins to be lost to the surroundings, allowing the fluid to condense. The condensate at **point(3)** is then expanded through a throttling valve to a low – pressure at state **point(4)** and enters the evaporator where it is evaporated to produce the necessary cooling effect . Then some of the evaporated vapour at **point(5)** is entrained by the ejector and the remainder at **point(6)** is absorbed by the strong lithium – bromide solution coming from the generator **(10**) via the solution heat exchanger **(11)** and a throttling valve **(12)** to form a weak

lithium – bromide solution at state **point(7)** . The heat produced by this absorption process is rejected to the environment. Finally the weak lithium – bromide solution at state **point(7)** is pumped back to the generator at state **point(9)** via the solution heat exchanger . Thus gaining sensible heat from the strong lithium – bromide solution returning to the absorber and hence completing the cycle.

The location of the ejector in the **(EARS)** is between the generator and condenser , where the ejector entrains some amount of the evaporated vapour from the evaporator that is mixed with the primary fluid coming from the generator in the mixing chamber , after that it is passing through the diffuser and from there to the condenser .

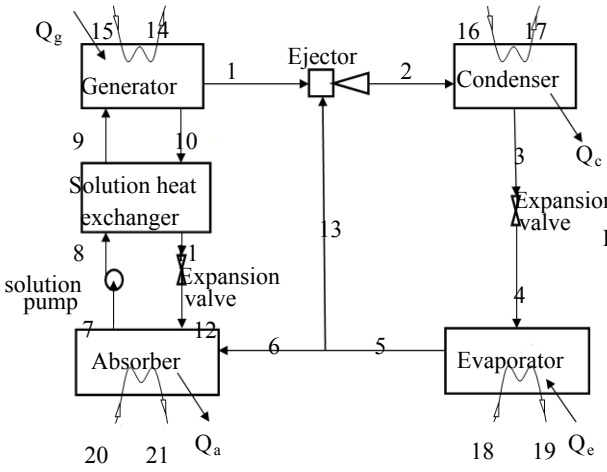

Figure(1) The schematic of the(EARS)

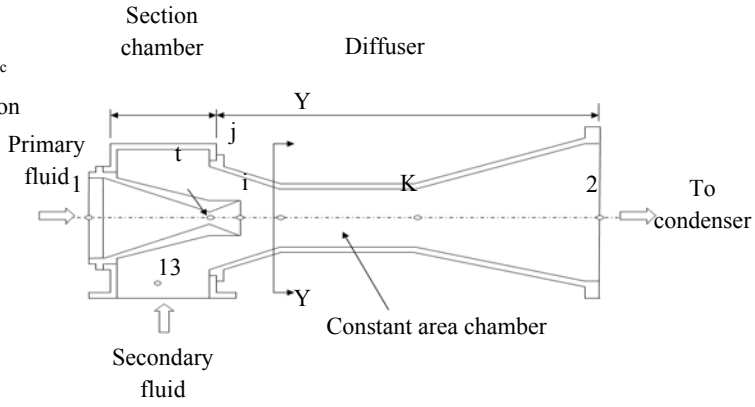

Figure(2) Ejector structure

3. Theoretical analysis and design of the (EARS)

3-1 Absorber

The mixing process of the absorbent and the refrigerant vapour generate latent heat of condensation and raise the solution temperature. Simultaneous with the developmental processing of latent heat, heat transfer with cooling water will then decrease the absorber temperature and , together with the solution temperature, creates a well blended solution that will be ready for the next cycle .

The energy balance in the absorber is :

$$Q_a = \dot{m}_6 h_6 + \dot{m}_{12} h_{12} - \dot{m}_7 h_7 = \dot{m}_{20} . Cp_W (T_{21} - T_{20}) \quad \ldots(1)$$

and the amount of heat transfer in the absorber is given by :

$$Q_a = U_a A_a \Delta T_{mla} \quad \ldots(2)$$

The following equation are used to evaluate the Log-mean temperature difference for the absorber [5] :

$$\Delta T_{mla} = \frac{(T_{12} - T_{21}) - (T_7 - T_{20})}{Ln \frac{(T_{12} - T_{21})}{(T_7 - T_{20})}} \quad \ldots(3)$$

The temperature of the absorber is expressed as [6] :

$$T_7 = T_{20} + T_{pinch,a} \quad \ldots(4)$$

Where ,

$$T_{pinch} = T_{ho} - T_{ci} \quad \ldots(5)$$

The mass and concentration balance for the strong and weak solution of the lithium bromide at the absorber can be expressed in the following equation :

$$\dot{m}_7 X_7 = \dot{m}_{12} X_{12} \quad \ldots(6)$$

By using EES External routines , the concentration of the lithium bromide weak solution that depart the absorber is determined at the absorber temperature and pressure which is calculated in the evaporator analysis . However, the concentration of the strong solution that get in the absorber is equal to the concentration of the lithium bromide that depart the generator. Also, the temperature of the solution get in the absorber is obtained at the concentration and pressure in that point , however the enthalpy for the solution that depart the absorber is obtained at the absorber temperature and the concentration of the weak solution .

3-2 Solution pump

A solution pump will mainly circulate and lift the solution from the lower pressure level side to the higher pressure level side of the system .

The power required to lift the solution from the lower pressure level side to the higher pressure level side is [7] :

$$W_{pump} = \frac{\dot{m}_7 \cdot v_7 \cdot (P_8 - P_7)}{\eta_{pump}} \quad \ldots (7)$$

The energy balance across the solution pump can be expressed as :

$$\dot{m}_7 . h_7 + W_{pump} = \dot{m}_8 . h_8 \quad \ldots (8)$$

The specific volume of the solution get in the solution pump is obtained by using EES External routines according to its concentration and temperature , while the temperature of the solution depart the pump is also obtained at the concentration and the enthalpy .

3-3 Solution heat exchanger

$$Q_{shx} = \dot{m}_{10} . (h_{10} - h_{11}) = \dot{m}_8 . (h_8 - h_8) \quad \ldots (9)$$

The area and the Log-mean temperature difference for the solution heat exchanger are calculated by using equations (2) & (3) at the corresponding information associated with the solution heat exchanger .

The temperature of the strong solution depart the solution heat exchanger is expressed in the following equation [5] :

$$T_{11} = T_8 . \varepsilon_{shx} + (1 - \varepsilon_{shx}) . T_{10} \quad \ldots (10)$$

The temperature and the enthalpy of the strong solution that depart the solution heat exchanger is obtained by using EES External routines .

3-4 Generator

The generator is a heat exchanger which generates vapour and extracts the refrigerant from the LiBr-water weak solution by the addition of the external heat from the heat source. The refrigerant vapour travels to the condenser while the LiBr-water strong solution is gravitationally settled at the bottom of the generator; the pressure difference between the generator and the absorber then causes it to flow out to the absorber through an expansion valve.

The energy balance equation in the generator is :

$$Q_g = \dot{m}_1 h_1 + \dot{m}_{10} h_{10} - \dot{m}_9 h_9 = \dot{m}_{14} \cdot Cp_g (T_{14} - T_{15}) \quad ...(11)$$

The area and the Log-mean temperature difference for the generator are calculated by using equations (2) & (3) at the corresponding information associated with the generator .

The concentration of the strong lithium bromide solution is evaluated by [7] :

$$X_{10} = X_7 + d_x \quad ...(12)$$

The generator temperature and the enthalpy of the strong solution depart the generator are obtained by using EES External routines .

3-5 Ejector

The analysis is based on the following assumptions :

1.The primary and the secondary fluids are typically based on the theoretical expression of ideal gas dynamics .

2.The primary and the secondary fluids have the same molecular weight and ratio of specific heats .

3.Mixing of the primary and the secondary fluids starts at the onset of the constant – area section .

4.The unity mach number is assumed at the throats of the nozzle and the diffuser .

5.Friction and mixing loss is accounted in the form of isentropic efficiency for the nozzle and the diffuser .

6.Kinetic energy of the inlet and outlet flows is not considered .

The pressure at the throat of the nozzle is calculated from the following equation [8]:

$$P_t = P_g \left(1 + \frac{k-1}{2}\right)^{\frac{k-1}{k}} \quad ...(13)$$

The velocity of the refrigerant at the throat of the nozzle can be expressed as :

$$V_t = \sqrt{2.\eta_N .(h_1 - h_{t,is})} \quad ...(14)$$

The entropy , the enthalpy and the specific volume of the refrigerant at the throat of the nozzle are obtained by using EES External routines .

The refrigerant mass flux through the throat of the nozzle is expressed as [8] :

$$G_t = \frac{V_t}{v_t} \quad ...(15)$$

The secondary refrigerant mass flux at section (y-y) , as shown in **figure (2)** , can be calculated in a similar way that expressed in the nozzle . By known the temperature and the pressure of the evaporator (T_e , P_e) , the pressure of the secondary refrigerant at section (y-y) can be calculated [8] :

$$P_{sy} = P_e \left(1 + \frac{k-1}{2}\right)^{\frac{k}{k-1}} \quad ...(16)$$

The velocity of the secondary refrigerant at section (y-y) can be expressed as [8] :

$$V_{sy} = \sqrt{2.\eta_N.(h_{13} - h_{sy,is})} \quad ...(17)$$

The mass flow coming from generator and passing through the convergent – divergent nozzle at choking condition can be calculated **from** [8] :

$$\dot{m}_p = P_g.a_t.\sqrt{\frac{\eta_N\, k}{T_g R}\left(\frac{2}{k+1}\right)^{\left(\frac{k+1}{k-1}\right)}} \quad ...(18)$$

In order to calculate the diameter at the nozzle inlet ($\mathbf{D_1}$) , the velocity is assumed very small thus by using the equation of the mass balance between the inlet and the throat of the nozzle we can obtained the area at the nozzle inlet :

$$\rho_1 V_1 a_1 = \rho_t V_t a_t \quad ...(19)$$

The density of the refrigerant at **point (1)** and at the throat of the nozzle is obtained by using EES External routines and the length of the convergent nozzle is evaluated by [9] :

$$L_1 = \frac{D_1 - D_t}{2.\tan\theta_1} \quad ...(20)$$

In order to obtained the mach number of the fluid at the nozzle exit at state point (i) , as shown in **figure(2)** , we use the following equation [8] :

...(21)

$$"M"_{"i"} = \sqrt{(("2" "\eta"_{" N"})/"k-1" "[1-" [("P"_{" i"} /"P"_{"1"})^{"k-1" /"k"}]])}$$

The pressure and the cross sectional area at the nozzle exit are evaluated by using the following equations [8] :

$$P_1 = \frac{P_1}{\left(1+\frac{k-1}{2}M_1^2\right)^{\frac{k}{k-1}}} \quad ...(22)$$

$$a_1 = \frac{a_T}{M_1}\left[\frac{2}{k+1}\left(1+\frac{k-1}{2}M_1^2\right)\right]^{\left(\frac{k+1}{2(k-1)}\right)} \quad ...(23)$$

The length of the divergent nozzle is evaluated by [9]:

$$L_2 = \frac{D_1 - D_t}{2.\tan\theta_2} \quad ...(24)$$

The velocity of the refrigerant at the nozzle exit can be expressed as :

$$T_1 = T_1 - \frac{V_1^2}{2.Cp} \quad ...(25)$$

The mach number of the primary flow at cross section(y-y) can be calculated from [8] :

$$\frac{P_{Py}}{P_1} = \left(\frac{1+\left(\frac{k-1}{2}\right)M_1^2}{1+\left(\frac{k-1}{2}\right)M_{Py}^2}\right)^{\frac{k}{k-1}} \quad ...(26)$$

The area of the primary flow at the section(y-y) is calculated by using the isentropic relation including an arbitrary coefficient (ϕ_g) , signifying loss in the flow point (1) to (y-y) section [8]:

$$a_{py} = a_1 \cdot \frac{\phi_g / M_{Py}}{1/M_1}\left(\frac{\frac{2}{k+1}\left(1+\left(\frac{k-1}{2}\right)M_{Py}^2\right)}{\frac{2}{k+1}\left(1+\left(\frac{k-1}{2}\right)M_1^2\right)}\right)^{\frac{(k+1)}{2(k-1)}} \quad ...(27)$$

The arbitrary coefficient for the primary flow (ϕ_g) leaving the nozzle can be assumed to be around (0.88) [10] .

The secondary flow rate at (y-y) section is illustrated as [8] :

$$\dot{m}_2 = P_{1g} \cdot a_{sy} \cdot \sqrt{\frac{\eta_N k}{T_{1g} R}\left(\frac{2}{k+1}\right)^{\left(\frac{k+1}{k-1}\right)}} \quad ...(28)$$

The secondary flow rate at (y-y) section is also obtained by using this equation [8] :

$$\dot{m}_2 = a_{sy} \cdot G_{sy} \quad ...(29)$$

Assuming that the entrained flow reaches choking conditions , the mach number of the secondary flow at section (y-y) is illustrated as [8] :

...(30)

"M" ₁"sy" " = " √("2" /"k-1" "[1-" ["(" "P" ₁"13" /"P" ₁"sy " ")"] ↑("k-1" /"k")])

A cross – sectional area at (y-y) is the summation of the area for primary flow (a_{py}) and entrained flow (a_{sy}) [8] :

$$a_k = a_{py} + a_{sy} \quad ...(31)$$

The temperature and the mach number of the streams at section (y-y) can be written as [8] :

$$\frac{T_1}{T_{Py}} = 1 + \frac{k-1}{2} M_{Py}^2 \quad ...(32)$$

$$\frac{T_{13}}{T_{sy}} = 1 + \frac{k-1}{2} M_{sy}^2 \quad ...(33)$$

The mass conservation law of impulse can be written as [8] :

$$\phi_m (m_P \cdot V_{Py} + m_s \cdot V_{sy}) = (m_P + m_s) \cdot V_m \quad ...(34)$$

An arbitrary coefficient accounting for friction loss (Φ_m) , varies with the ejector area ratio (a_k/a_t) and it is obtained by using this equation [8] :

$$\phi_m = 1.037 - 0.02857 \cdot \frac{a_k}{a_t} \quad ...(35)$$

The length of the mixing section is generally defined in terms of the throat diameter , for steam jet ejectors , the recommended lengths are different , depending on the research . However , all of them are in the range of (6 – 10) times the throated diameter [8] :

$$L_3 = 6 \cdot D_k \quad ...(36)$$

The length of the subsonic conical diffuser can be written as :

$$L_4 = \frac{D_2 - D_k}{2 \tan \theta_3} \quad ...(37)$$

The total length of the diffuser can be expressed as :

$$L_d = L_3 + L_4 \quad ...(38)$$

The velocities of the primary and secondary flows at section (y-y) can be expressed as [8] :

$$V_{Py} = M_{py} \cdot \sqrt{k \cdot R \cdot T_{Py}} \quad ...(39)$$

$$V_{sy} = M_{sy} \cdot \sqrt{k \cdot R \cdot T_{sy}} \quad ...(40)$$

In order to obtained the temperature at the mixing point (T_m) , the energy balance at the mixing point can be expressed as [8] :

$$\dot{m}_p\left[C_p T_{py}+\frac{V_{py}^2}{2}\right]+\dot{m}_s\left[C_p T_{sy}+\frac{V_{sy}^2}{2}\right]=(\dot{m}_p+\dot{m}_s)\left[C_p T_m+\frac{V_m^2}{2}\right] \quad ...(41)$$

The enthalpy at the mixing point is obtained by using the equation [8] :

$$h_m = C_p T_m+\frac{V_m^2}{2} \quad ...(42)$$

The mach number of the mixing point is obtained by :

$$M_m = V_m / \sqrt{k.R.T_m} \quad ...(43)$$

Assuming that the mixed flow after the shock undergoes an isentropic process , the pressure of the mixed flow from the mixing point to point (k) is constant at (P_k) :

$$P_k = P_m .\left[1+\frac{2k}{k+1}\left(M_m^2-1\right)\right] \quad ...(44)$$

The mach number of the mixing point is obtained by using this equation [8] :

$$M_k^2 = \frac{1+\left(\frac{k-1}{2}\right)M_m^2}{kM_m^2-\left(\frac{k-1}{2}\right)} \quad ...(45)$$

The temperature of the refrigerant stream at **point (k)** is obtained by using this equation :

$$M_k = V_k / \sqrt{k.R.T_k} \quad ...(46)$$

While the velocity of the refrigerant stream at **point (k)** be estimated as :

$$h_m+\frac{V_m^2}{2} = h_k+\frac{V_k^2}{2} \quad ...(47)$$

The enthalpy of the refrigerant stream at **point (k)** is obtained by using EES built in thermophysical property functions , with the pressure and temperature known .

The enthalpy of the refrigerant stream at the exit of the ejector can be estimated as :

$$h_2 = h_k+\frac{V_k^2}{2} \quad ...(48)$$

While the velocity of the refrigerant stream at the exit of the ejector can be estimated as :

$$T_2 = T_k+\frac{V_k^2}{2.C_p} \quad ...(49)$$

The cross sectional area at the exit of the diffuser can be depicted as :

$$a_2 = a_k . \frac{1}{\sqrt{M_2}}\left[\frac{2+(k-1)M_2^2}{k+1}\right]^{\frac{k+1}{4(k-1)}} \quad ...(50)$$

The mach number at point (2) is given by :

$$M_2 = V_2 / \sqrt{k.R.T_2} \quad ...(51)$$

The velocity of the refrigerant stream at **point (2)**is given by the following equation :

$$\dot{m}_p h_1 + \dot{m}_s h_{15} = (\dot{m}_p + \dot{m}_s)\left(h_2 + \frac{V_2^2}{2}\right) \quad ...(52)$$

The pressure lift in the diffuser can be estimated as [8] :

$$P_3 = P_k \left(\frac{\eta_d (k-1)}{2} M_k^2 + 1\right)^{\frac{k}{k-1}} \quad ...(53)$$

The entrainment ratio (ω) can be written as [8] :

$$\omega = \frac{\dot{m}_s}{\dot{m}_p} \quad ...(54)$$

3-6 Condenser

The energy balance in the condenser is :

$$Q_C = (\dot{m}_1 + \dot{m}_p)(h_2 - h_3) = \dot{m}_{16} . Cp_W (T_{17} - T_{16}) \quad ...(55)$$

The area and the Log-mean temperature difference for the condenser are calculated by using **equations (2)** , **(3)** at the corresponding information associated with the condenser .

The condenser temperature is expressed as [6] :

$$T_3 = T_{16} + T_{pinch,c} \quad ...(56)$$

The enthalpy of the refrigerant (water vapour) at the exit of the condenser are obtained by using EES built in thermophysical property functions .

3-7 Evaporator

The energy balance in the evaporator is :

...(57)

| "m"₁"8" "). (" "h" ₁"5" "-" "h" ₁"4" ")" " = " "m" ₁"10" "." [" "Cp"] ₁"w" "(" "T" ₁"10" "-" "T" ₁"19" ")"

The area and the Log-mean temperature difference for the evaporator are calculated by using **equations (2)** , **(3)** at the corresponding information associated with the evaporator .

The evaporator pressure , temperature and dryness fraction of the refrigerant entering the evaporator , and the enthalpy of the refrigerant leave the evaporator are obtained by using EES built in thermophysical property functions .

3-8 Crystallization problem

Aqueous lithium bromide is a salt solution substance where the salt component will start to precipitate when the mass fraction of salt exceeds the maximum allowed of solution solubility .

The crystallization problem appears when the absorption refrigeration system is off and the flow is stopped due to a significant temperature drop ; during the operating stage , crystallization tends to occur at the outlet of the solution heat exchanger where temperatures are relatively low and mass fractions are high .

A complete mixing process between refrigerant and absorbent in the absorber is one of the main keys to preventing crystallization because the salt fraction is completely mixed with the refrigerant preventing the saturation of liquid solubility . A complete mix of refrigerant and absorbent is controlled by the heat rejection process in the absorber so the absorber temperature is maintained at the design condition .

The coefficient of performance of the (**CARS**) using lithium bromide-water as a working solution can be improved by reducing the condenser and absorber temperatures or increasing the generator and evaporator temperatures . However , the temperature of the condenser and the absorber depend on the cooling fluid available , and the temperature of evaporator depends on the refrigerating temperature requirement . Thus , the coefficient of performance can be maximized only by raising the generator temperature . However , even if a high-temperature heat source is available , the generator temperature , normally , cannot be increased beyond the solution saturation temperature . Lithium bromide solution is saturated at a concentration around 70%. If the solution is already saturated , reducing the pressure or increasing the temperature , crystallization will occur, and the system can no longer be operated [11] .

If an ejector using high-pressure steam from the generator as the primary fluid is introduced between the condenser and the generator , the cycle can be operated with the generator pressure higher than that in the condenser . If a high-temperature heat source is available , the generator temperature may be raised and the solution concentration can be maintained constant and the crystallization problem is not occur .

Dong-Seon Kim [12] did a polynomial fit for solubility of pure lithium bromide in water and groups it in four regions :

Region I , $X_{strong}<48.5\%$

$$T_{crit} = -398.3 + 25.107\ X_{strong} - 0.253\ X_{strong}^2 \quad ...(58)$$

Region II , $48.5< X_{strong[]}<57.2\%$

$$T_{crit} = -919.4 + 38.51957477\ X_{strong} - 0.3080928653\ X_{strong}^2 \quad ...(59)$$

Region III, $57.2< X_{strong[]}<65.5\%$

$$T_{crit} = -1159.4 + 42.7386184\ X_{strong} - 0.308288545\ X_{strong}^2 \quad ...(60)$$

Region IV , $X_{strong}>=65.5\%$

$$T_{crit} = -2046.536869 + 58.34181996\ X_{strong} - 0.3391180069\ X_{strong}^2 \quad ...(61)$$

3-9 System performance

The overall energy balance equation for the whole system will be :

$$Q_g + Q_e + W_{pump} - Q_c - Q_a = 0 \quad ...(62)$$

The coefficient of performance for the both (**CARS**) and (**EARS**) is given by :

$$COP = \frac{Q_e}{Q_g + W_{pump}} \quad ....(63)$$

4. Results and Discussion

A comparison between the conventional absorption refrigeration system (**CARS**) and a combined ejector – absorption refrigeration system (**EARS**) is illustrated in **figure (3)** . It can be seen that as the mass flow of the steam inlet to the generator increase , the generator surface area required decrease , because when the mass flow of steam inlet to the generator increase , the temperature of the steam leave the generator increases , and hence the Log-mean temperature difference increases and the generator surface area decreases according to **equation (2)** .

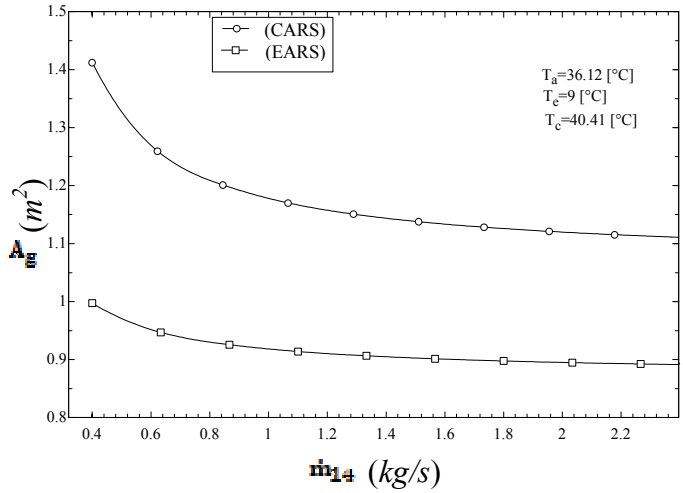

Figure(3) The effect of the steam mass flow on the generator surface area for both system.

Figure (4) shows the variation of generator surface area with the mass flow rate of the LiBr – H_2O weak solution for the (**CARS**) and the (**EARS**) . The figure shows that the generator surface area for the (**EARS**) is less than that for the (**CARS**) , this is because the heat source temperature of the (**EARS**) is higher than that for the (**CARS**) which is led to increase the Log – mean temperature difference for the generator and hence the generator surface area is reduced .

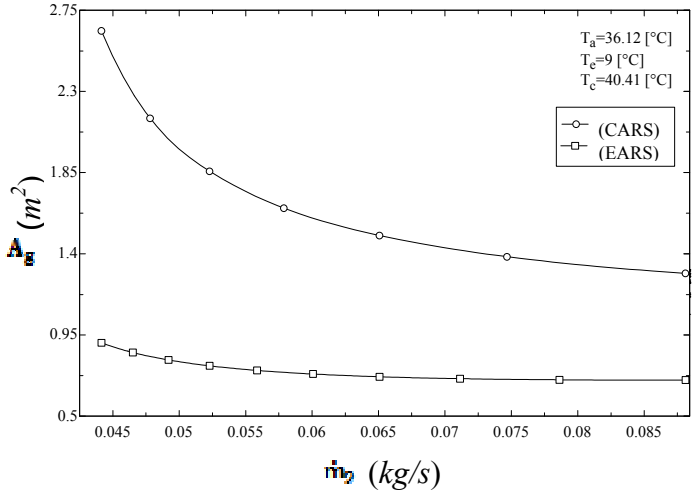

Figure(4) The effect of the weak solution mass flow on the generator surface area for both system.

The effect of the generator pressure on the ejector area ratio (a_k/a_t) is illustrated in **figure(5)** , where the area ratio (a_k/a_t) increase as the generator pressure and entrainment ratio increased , therefore the relationship between the area ratio and the pressure is linear as shown , since when the generator pressure is increased , the throat diameter of the nozzle

decreases according to the **equation (18)** for a certain entrainment ratio and this will lead to increase the area ratio (a_k/a_t) .

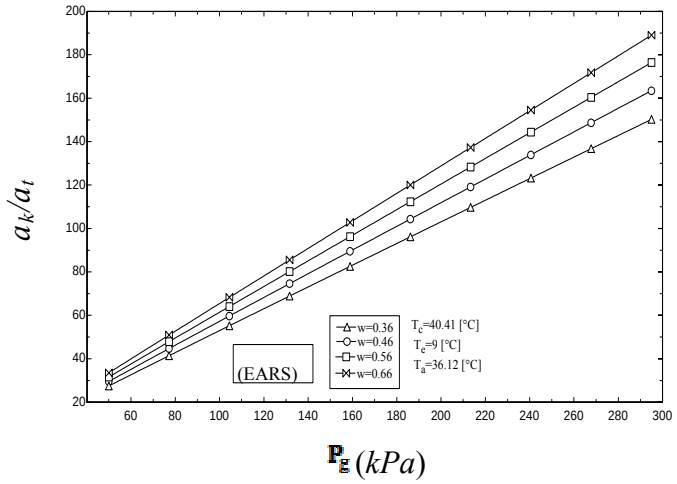

Figure(5) The effect of generator pressure on the area ratio.

Also , the area ratio is reduced by increasing the evaporator pressure ، because when the evaporator pressure increased the mass flow rate of the secondary refrigerant coming from the evaporator is also increased , and this caused by increasing the primary refrigerant for a certain entrainment ratio and this guide to increase the throat area of the nozzle (a_t) according to **equation (18)** and hence reduce the area ratio (a_k/a_t) as shown in **figure (6)** .

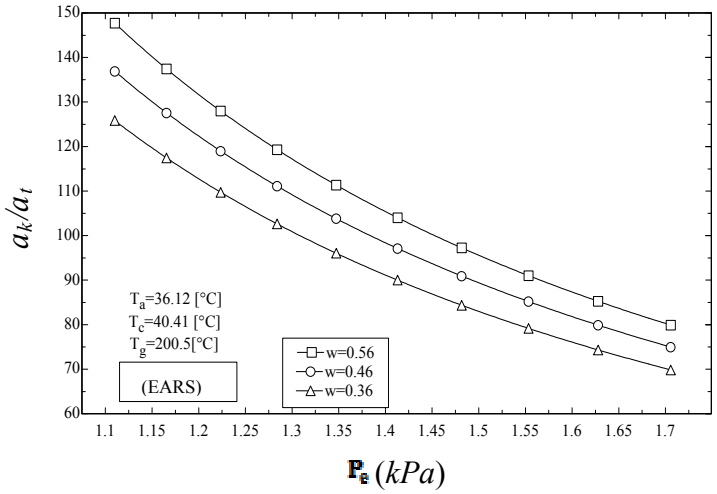

Figure(6) The effect of evaporator pressure on the area ratio.

Figure (7) showed the evaporator surface area as a function of the chilled water mass flow for the (**CARS**) and the (**EARS**) at the same chilled water inlet temperature (***T*$_{18}$**) . It is illustrated that the evaporator surface area for the **(EARS**) is larger than that for the (**CARS**)

because the cooling effect is increased for the (**EARS**) due to the increasing of the refrigerant flow rate through the evaporator .

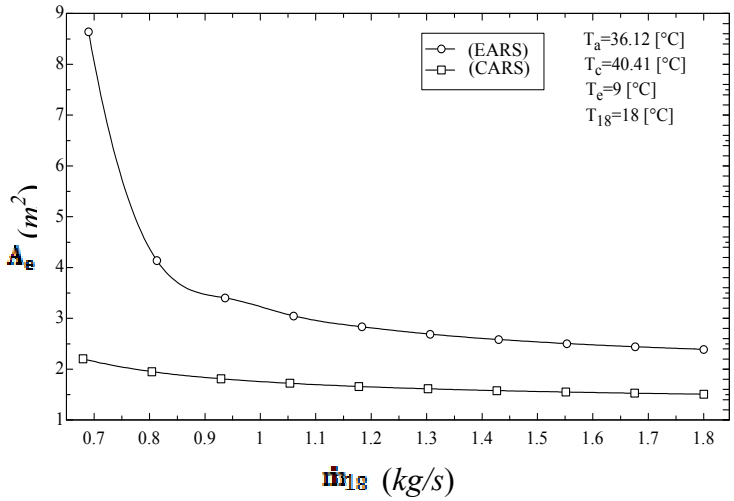

Figure(7) The effect of the chilled water mass flow on the evaporator surface area for both system.

Whereas **figure (8)** explain the effect of the mass flow rate of the weak solution on the area of the absorber for both **(EARS**) and (**CARS)** . It is noted that the increase of the mass flow rate of the weak solution caused by increasing the absorber surface area at constant absorber temperature .

The increasing of the mass flow rate of the weak solution entering the generator will lead to reduce the concentration of the strong solution and this mean that a small amount of the refrigerant vapour can be absorbed by the strong solution in the absorber in order to reduce its concentration and reach it to the condition of the weak solution . Therefore the refrigerant mass flow through the condenser and evaporator is decreased and thus reducing the cooling effect and the coefficient of performance .

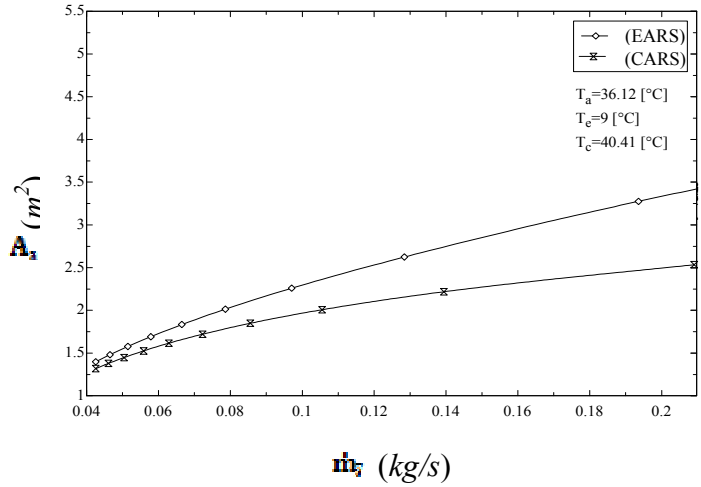

Figure(8) The effect of the weak solution mass flow on the absorber surface area for both system.

Figure (9) indicated that the values of the coefficient of performance for the (**EARS**) are higher than that for the (**CARS**) . This is due to the existence of the ejector that caused by increasing the refrigerant mass flow in the evaporator , hence the cooling effect of the evaporator is increased and as a result , the coefficient of performance is increased .

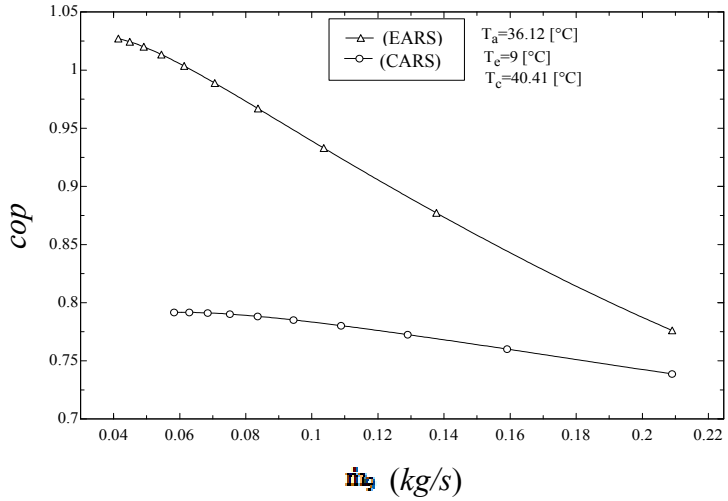

Figure(9) The effect of the weak solution mass flow on the COP for both system.

The variation of the coefficient of performance with generator temperature is illustrated in **figures (10)** , (**11**) , and **(12)** . In all cases , it can be seen that as the generator temperature increases , the coefficient of performance will increase . To interpret this increasing in the coefficient of performance , it can be said that the increasing in the generator temperature caused by increasing the concentration of the strong solution and holding the mass flow rate and concentration of the weak solution constant resulting in a reduction in the mass of the strong solution and hence the heat input to the generator is reduced which leads to a higher

coefficient of performance . In addition , the (**EARS**) operates at a higher generator temperature and pressure as compared with that of the (**CARS**) . The higher pressure causes the ejector inlet pressure to increase and the pressure at the throat is also increased , then the shock advancing downstream the nozzle exit , and the flow in the divergent section of the nozzle is entirely supersonic . This caused by increasing the vacuum at the nozzle exit , resulting in large pressure difference between the mixing section and the evaporator . Therefore , the mass flow of the sucked vapour will increase and as a result the cooling effect will increase and hence the coefficient of performance will improve as shown in **figure (13)** .

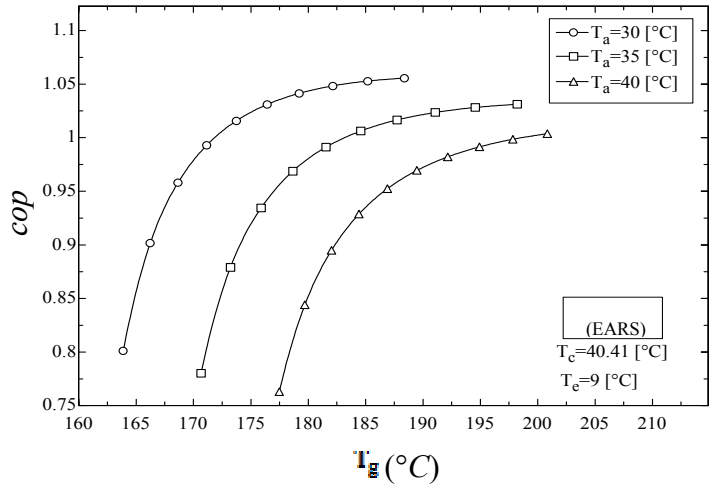

Figure(10) The effect of generator temperature on COP under different absorber temperatures.

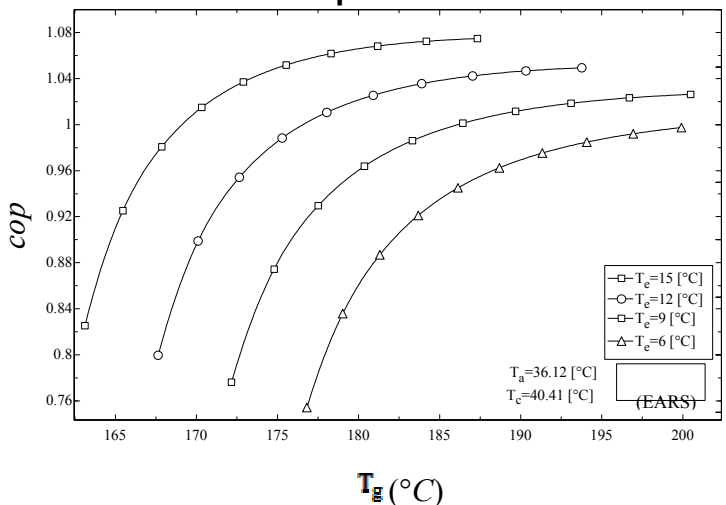

Figure(11) The effect of generator temperature on COP under different evaporator temperatures.

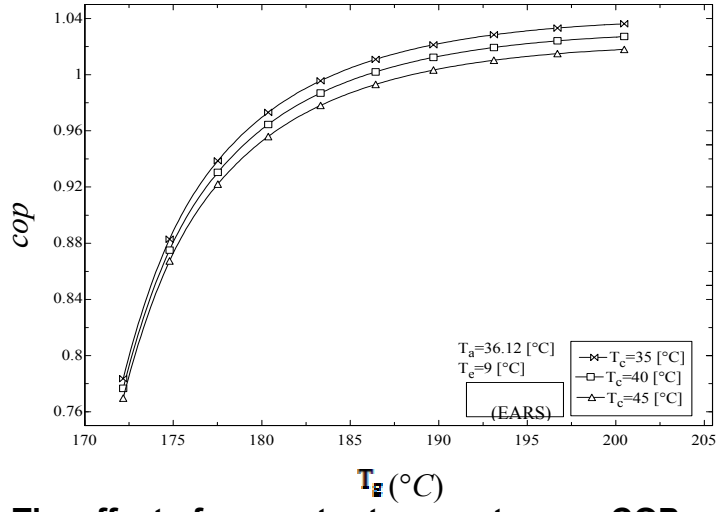

Figure(12) The effect of generator temperature on COP under different condenser temperatures.

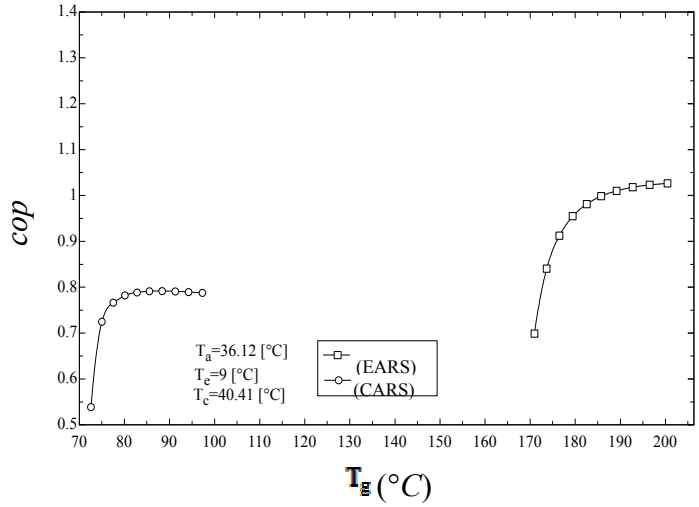

Figure(13) The comparison of the performance between CARS and EARS under the variation of the generator temperature.

Figure (14) showed the effect of the condenser temperature variation on the coefficient of performance for both **(EARS)** and **(CARS)** . For (**CARS)** , the pressure of the condenser and generator will increase when the condenser temperature is increased . This will require higher generator temperature in order to vaporize a certain amount of refrigerant , and as the temperature of the generator is originally constant , therefore the amount of the refrigerant that vaporized in the generator will reduce as the condenser temperature increased . This is caused by reducing the coefficient of performance . Also , in **(EARS)** , it can be seen that the performance of the system suffers with an increase in condensing temperature . Since the

condenser pressure is increases as the condenser temperature increases , the back pressure of the ejector will increase . This caused by moving the shock out of the nozzle . **i.e** the pressure in the mixing section is increased and the pressure difference between the evaporator and the mixing section will decreased , resulting in a reduction in the suction flow and then the coefficient of performance is decreased .

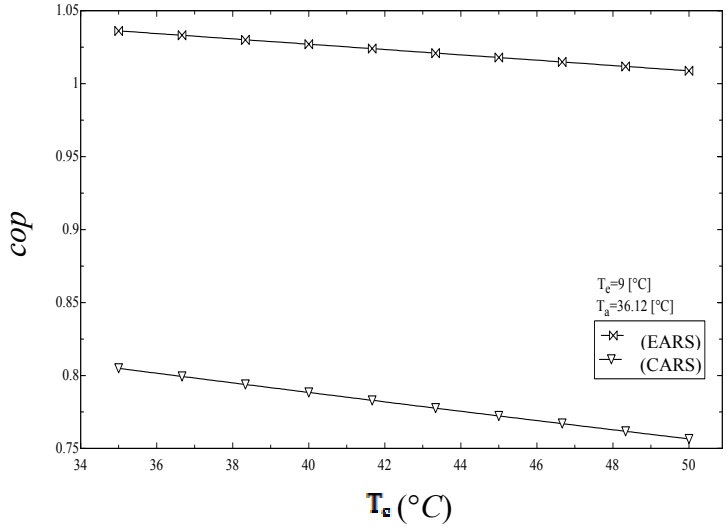

Figure(14) The comparison of the performance between CARS and EARS under the variation of the condenser temperature.

A comparison of the evaporator temperature effect on the coefficient of the performance for the ***(CARS***) and the (***EARS***) is illustrated in **figure (15)** . In the **(CARS)** , the pressure of evaporator and absorber will increase when the evaporator temperature increased and hence the concentration of the weak solution is reduced and this means that the amount of refrigerant will reduce while the concentration of the strong solution remains constant in the generator and caused by reducing the amount of the strong solution that leave the generator and as a result the heat energy required is reduced . It can be concluded that the coefficient of performance increases when the evaporator temperature increased .

The coefficient of the performance for the **(EARS)** is also increased when the evaporator temperature increased for the same reason mentioned above . In addition , when the evaporator temperature is increased its pressure increased and hence increase the velocity of the secondary refrigerant stream which is leads to increase the entrainment ratio and the refrigerant vapour mass flow rate through the condenser and the evaporator leading to

increase the coefficient of performance for the system . Therefore we notice that the coefficient of performance for the (**EARS)** is higher than that for the (**CARS**).

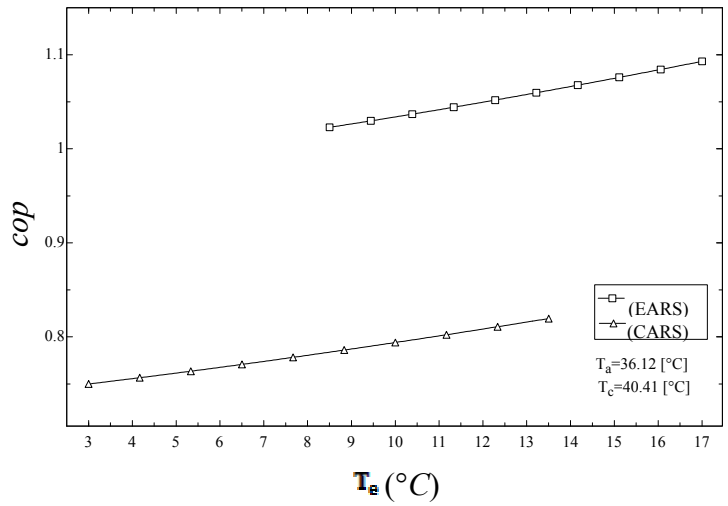

Figure(15) The comparison of the performance between CARS and EARS under the variation of the evaporator temperature.

Figure (16) shows the effect of the absorber temperature on the coefficient of performance for both systems . It can be seen that , when the temperature increased concentration of the weak solution in the absorber will be increased . Therefore more solution is required to produce a certain amount of refrigerant vapour for the same amount of the strong solution leaving the generator and hence larger amount of heat energy is required in the generator . As a result , the coefficient of performance is increased as the absorber temperature increases . Also , it can be noted that the performance of the (**EARS**) is higher than that for the (**CARS**) . This is due to the increase in the amount of refrigerant flow rate through the evaporator in the (**EARS**) .

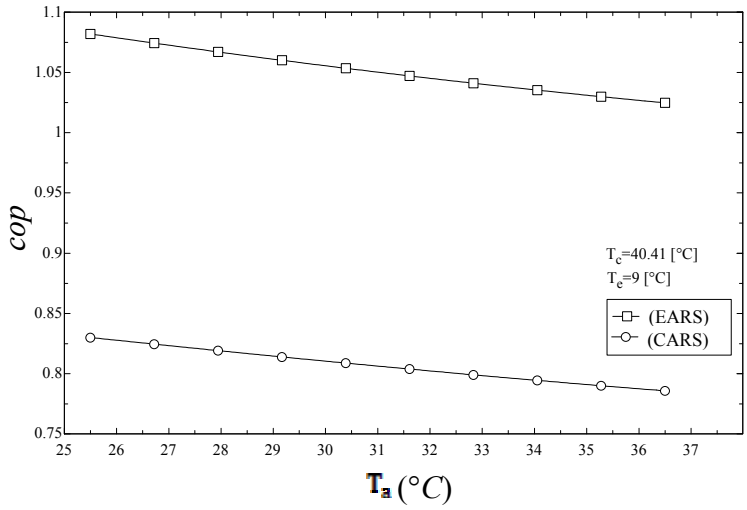

Figure(16) The comparison of the performance between CARS and EARS under the variation of the absorber temperature.

A comparison between the (**EARS**) and the (**CARS**) is illustrated in **figure (17)** , it shows the effect of the temperature of the cooling water entering the absorber on the coefficient of performance. when the temperature of the cooling water increased the absorber temperature is also increased according to **equation (4)** so that the coefficient of performance will decrease.

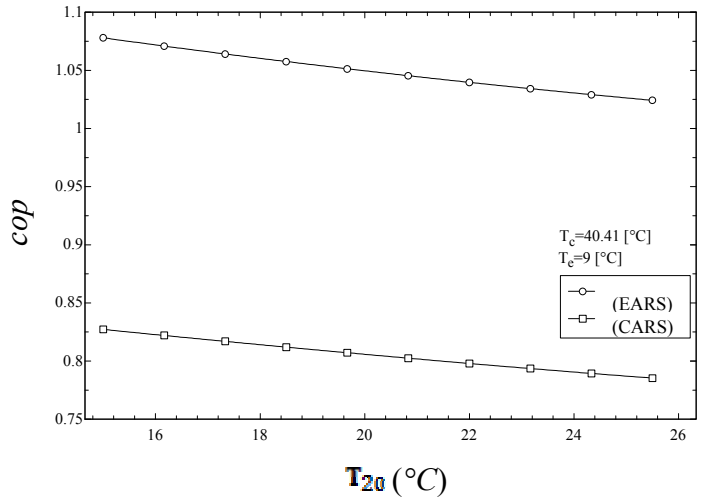

Figure(17) The comparison of the performance between CARS and EARS under the variation of the cooling water temperature.

Figure (18) showed the variation of the coefficient of performance with the absorber pinch temperature . It can be seen that as the pinch temperature increases , the absorber temperature is also increased and hence the coefficient of performance will decrease for both (**EARS**) and **(CARS**) system , but the performance for the (**EARS)** is higher . This is due to the increase of the refrigerant flow rate passing through the evaporator .

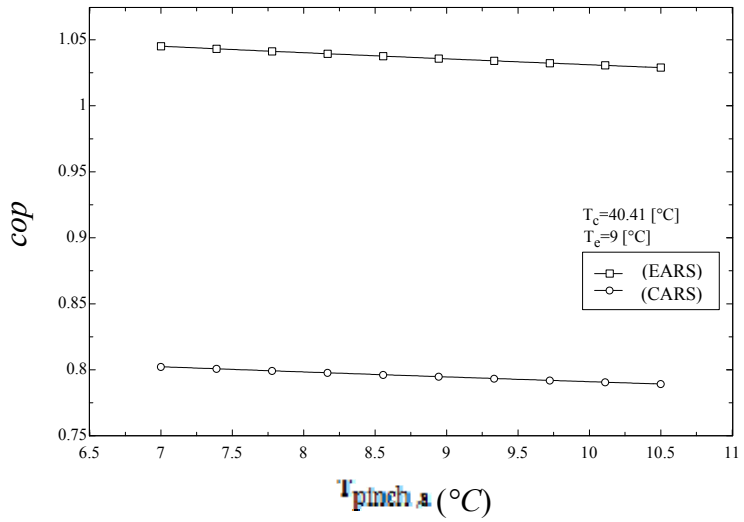

Figure(18) The comparison of the performance between CARS and EARS under the variation of the absorber pinch temperature.

The coefficient of performance for the **(EARS)** extremely depends on the entrainment ratio of the ejector . The effect of the entrainment ratio on the coefficient of performance is illustrated in **figure (19)** . It can be noted that the coefficient of performance will increase with the increase of the entrainment ratio . This is because the increase of this ratio will lead to increase the mass flow rate of the secondary refrigerant for fixed mass flow of the primary refrigerant , since the mass flow rate passing through the condenser and evaporator is increased and the cooling effect is also increased , so that the coefficient of performance will increase .

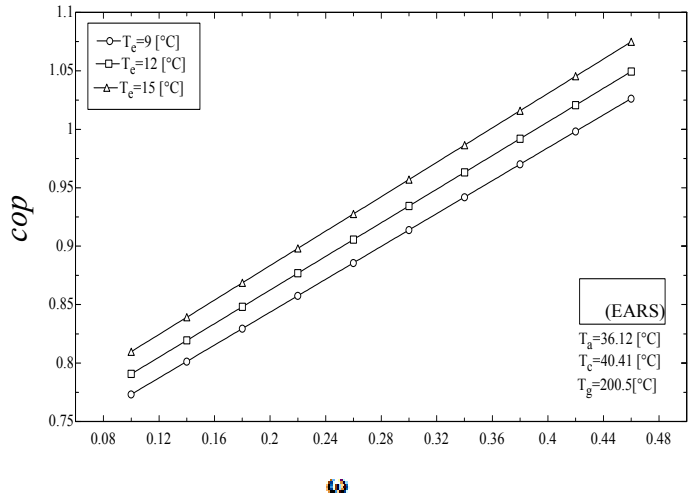

Figure(19) The effect of entrainment ratio on COP under different evaporator temperatures.

The problem of crystallization is an important factor to monitor for a water-lithium bromide absorption system because it might affect the operation and the lifetime of the absorption system . Crystallization tends to occur between the expansion valve and the absorber where the pressure level is low enough and the solution temperature is close to the crystallization line . A higher concentration difference means the fraction of lithium bromide at the outlet of the generator is high and more of the water fraction is extracted from the low weak solution as a refrigerant . Since the solubility limit is a strong function of mass fraction and temperature, the salt substance of aqueous lithium bromide solution tends to precipitate easily at a higher solution concentration. It is important to keep the solution temperature above and not allow it to go below the crystallization temperature line. As seen in **Figure (20)**, the temperature along the expansion valve and absorber was monitored since the crystallization process appears most at this part of the lithium bromide absorption system .

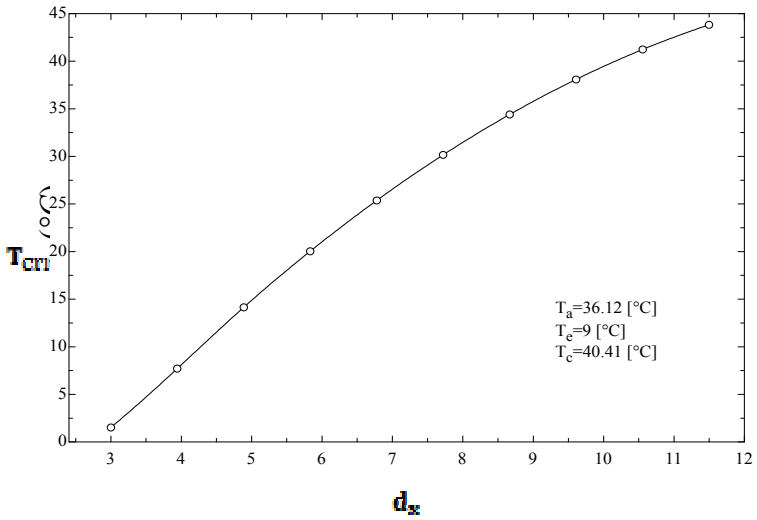

Figure(20) The effect of the strong–weak solution concentration difference on the critical strong solution temperature.

It can be concluded that , the addition of the ejector caused by increasing the coefficient of performance by about (30.35%) and prevent the crystallization to be occurred .

Table (1) shows the results of the design of the ejector , while **table (2)** shows the results of the design of the heat exchangers for the (**EARS**) and the (**CARS**) .

Table(1) : the results of the design of the ejector

description	symbol	value	unit
Entrainment ratio	ω	0.46	———
Mass flow of primary refrigerant from the generator.	${}_p\dot{m}$	0.007487	*kg/s*
Mass flow of secondary refrigerant from the evaporator.	${}_s\dot{m}$	0.003444	*kg/s*
diameter at the nozzle inlet.	D_1	0.025	*m*
Diameter of the throat of the nozzle.	D_t	0.0032	*m*
Diameter at the exit of the nozzle.	D_i	0.009674	*m*
Diameter of the mixing section.	D_k	0.03655	*m*
Diameter at the exit of diffuser.	D_2	0.08059	*m*
The length of the convergent nozzle.	L_1	0.01299	*m*
The length of the divergent nozzle.	L_2	0.02303	*m*
The length of the mixing section.	L_3	0.2192	*m*
The length of the subsonic conical diffuser.	L_4	0.1567	*m*
The total length of the diffuser.	L_d	0.376	*m*

Table(2) : the results of the design of the heat exchangers for the (EARS) and the (CARS)

description	value		unit
	(CARS)	(EARS)	
Generator surface area.	1.292	0.9593	m^2
Absorber surface area.	1.871	1.399	m^2
Solution heat exchanger surface area.	0.4541	0.1491	m^2
Condenser surface area.	1.692	2.581	m^2
Evaporator surface area.	1.755	3.195	m^2

5. References :

1. Wu .S , BEng, MSc ," **Investigation of ejector re-compression absorption refrigeration cycle"** , Thesis submitted to the University of Nottingham for the degree of Doctor of Philosophy, May, 1999.

2. Zong-Chang and Jian-wei , **"Analysis of thermodynamic performance of combined ejection-absorption heat pump with LiBr-H_2O",** Journal of Dalian University of Technology , vol.48 , no.4 ,PP(480-485) , July , 2008.

3. Ereira A.F,"Study **of a liquid-vapour Ejector in context of an advanced TPL ejector-absorption cycle working with a low temperature heat source and an ammonia-water mixture"** , int.comm. , 2009.

4. Hong D. ,Chen G. , Tang L. , and He .Y ,"**A novel ejector-absorption combined refrigeration cycle" ,** International Journal of Refrigeration ,Vol.XXX , PP(I-8) , 2010.

5. Holman J.P. , **"Heat transfer"** , 8th edition , Mc graw-Hill , Inc. ,1999.

6. Björnsdòttir U. ,"**Use of Geothermal Energy for Cooling**" , Ph.D. Thesis , University of Iceland , June ,2004.

7. Tesha , "**Absorption Refrigeration System as an integrated condenser cooling unit in geothermal power plant"**, M.SC Thesis , Department of mechanical and Industrial Engineering University of Iceland , 2009.

8. Pridasawas W. ,"**solar-driven refrigeration systems with focus on ejector cycle"** , Ph.D. thesis Submitted to Department of Energy Technology, School of Industrial Engineering and Management , Royal Institute of Technology KTH , Stockholm , 2006.

9.Al-saffawi Adnan M. ," **Computer aided design of an ejector cooler system"** . International Conference Refrigeration and Air-Conditioning , Amman-Jorden , 1985.

10. Huang , B.J. , Chang , J.M., Wang , L.P and Petrenko , U.A. ,"**A 1-D Analysis of Ejector performance"** , International Journal of Refrigeration , vol.22 , PP(354-364) , 1999.

11.Aphornratana .S and Eames W.I , "**Experimental investigation of a combined ejector-absorption refrigerator"** , International Journal of energy research , vol.22 ,PP(195-207) , 1998.

12.Kim ,D.S. **,"Solar absorption cooling",** Dissertation ,Delft University of Technology, 2007.